



HAL
open science

Why does spatial extrapolation of the vine water status make sense? Insights from a modelling approach

Sébastien Roux, Rémi Gaudin, Bruno Tisseyre

► To cite this version:

Sébastien Roux, Rémi Gaudin, Bruno Tisseyre. Why does spatial extrapolation of the vine water status make sense? Insights from a modelling approach. *Agricultural Water Management*, 2019, 217, pp.255-264. 10.1016/j.agwat.2019.03.013 . hal-02609250

HAL Id: hal-02609250

<https://hal.inrae.fr/hal-02609250>

Submitted on 26 Oct 2021

HAL is a multi-disciplinary open access archive for the deposit and dissemination of scientific research documents, whether they are published or not. The documents may come from teaching and research institutions in France or abroad, or from public or private research centers.

L'archive ouverte pluridisciplinaire **HAL**, est destinée au dépôt et à la diffusion de documents scientifiques de niveau recherche, publiés ou non, émanant des établissements d'enseignement et de recherche français ou étrangers, des laboratoires publics ou privés.



Distributed under a Creative Commons Attribution - NonCommercial 4.0 International License

1 Why does spatial extrapolation of the vine water status make 2 sense? Insights from a modelling approach

3
4 Sébastien Roux^{1,*}, Rémi Gaudin², Bruno Tisseyre³

5
6 1: MISTEA, INRA, Montpellier SupAgro, Univ Montpellier, Montpellier, France

7 2: SYSTEM, INRA, Montpellier SupAgro, CIRAD, Univ Montpellier, Montpellier, France

8 3: ITAP, INRA, IRSTEA, Montpellier SupAgro, Univ Montpellier, Montpellier, France

9 *: corresponding author

10
11
12

13 **Abstract**

14 This work is devoted to precision agriculture and more precisely to the spatial monitoring
15 of water status in viticulture. An empirical approach was introduced in 2008 based on the
16 extrapolation across a domain (vineyard block, vineyard, region) of vine water status
17 observations from a reference site using a simple statistical model, called SPIDER, and
18 proved efficient in many studies. Once the extrapolation model is calibrated, this approach
19 leads to a concentration of measurements for one site only (reference site) while providing
20 an estimate of the grapevine water status at a larger spatial scale. It is a promising hybrid
21 approach based both on regular (but targeted) measurements and on modelling. However,
22 so far only empirical guidelines for its practical use have been provided. Moreover, the
23 limits of validity (spatial, temporal, etc.) of such an approach are not known.

24 This work intends to use a mechanistic model based on grapevine water balance
25 modelling to study to what extent a simulated water status can be spatially extrapolated at
26 the field scale. The water balance model was calibrated on two datasets (different cultivars
27 and weather data) and used to analyse the performances of SPIDER. The results
28 confirmed the relevance of the empirical approach (SPIDER) based on water status spatial
29 extrapolation with a low error level on the two datasets studied. The use of the water
30 balance model also helped define the validity domain of SPIDER: it confirmed the
31 importance of having dominantly dry conditions and revealed the possibility of recovering
32 good prediction quality after strong rainfall or irrigation. This study globally demonstrates
33 the relevance of spatial extrapolation of the vine water status from a reference site with a

34 linear regression model and provides new insights on the properties of the predictions for
35 application in viticulture either at the within-field level or at larger scale.

36

37 **1. Introduction**

38 Several studies have shown that changes in grapevine water status (Ψ) have a direct
39 effect on grape composition and quality by influencing vegetative growth, fruit growth,
40 yield, canopy microclimate, and fruit metabolism (see among others, Tregoat et al., 2002;
41 Dry and Loveys, 1998; Van Leeuwen and Seguin, 1994; Ojeda et al., 2002; Brillante et al.,
42 2018). Characterizing the spatial variability of Ψ is then a key issue for terroir study
43 (Seguin, 1983; Van Leeuwen et al., 2009). The spatial monitoring of Ψ therefore provides
44 important information for managing and/or assessing grape quality (Van Leeuwen et al.,
45 2009; Rezaei and Reynolds, 2010). In a review paper, Acevedo-Opazo et al. (2008)
46 discussed the importance of methods for spatial monitoring of vine water status.
47 Furthermore, the same authors proposed an empirical spatial model (Eq. 1) to predict the
48 vine water status (estimated with the water potential Ψ) across a given domain (vineyard
49 block, vineyard, region, etc.).

$$50 \quad \Psi(s, t) = a_s \cdot \Psi(s_{ref}, t) \quad [\text{Eq.1}]$$

51 The principle of the model is to extrapolate a reference Ψ value $\Psi(s_{ref}, t)$ measured at a
52 reference site s_{ref} and time t . The extrapolation is based on a linear relationship defined by
53 the coefficients a_s whose values are specific to site s . The model provides an estimate
54 $\Psi(s, t)$ of Ψ values at any site s where a coefficient a_s is available. This spatial model has
55 been successfully tested at the within-field level (Acevedo-Opazo et al., 2010) and at a
56 vineyard level constituted of several blocks (Taylor et al., 2010). More recently, the model
57 has been successfully tested at the whole denomination scale by Baralon et al. (2012). At
58 this scale, the approach was called SPIDER (SPatial extrapolation of the vlne water status
59 at the whole DENomination scale from a Reference site). Although empirical, The SPIDER
60 approach may present several practical advantages: i) it relies solely on direct Ψ
61 measurements (i.e. leaf water potential), which can be performed by vine growers.
62 Therefore, the calibration of the model can be implemented within a conventional
63 monitoring of Ψ . The method does not require spatial estimates of other variables related
64 to soil or other environmental factors that may be difficult and expensive to measure; ii) the
65 model can also be calibrated from measurements that have already been taken.

66 Therefore, it makes it possible to use existing databases of Ψ (historical databases),
67 provided that the data are geo-located; and iii) the principle of the method allows to
68 consider asynchronous measurements when labor is the limiting factor, provided that the
69 measurement of Ψ is systematically done on the reference site.

70 Despite these practical advantages, the results obtained have highlighted a number of
71 limitations of SPIDER that the empirical approach allows to observe but does not allow to
72 quantify objectively. Two main limitations have been identified (Baralon et al., 2012); the
73 first one refers to the climatic context of the year used to calibrate the model. Indeed,
74 Baralon et al. (2012) stressed that the database used to calibrate the model must
75 necessarily include data with a large magnitude of water restriction which requires a
76 sufficiently long summer period without any rainfall to reach high Ψ values over the domain
77 under consideration. The second limitation relates to conditions concerning the soil,
78 climate and cultural practices that the study area must present so that the linear
79 relationship associating Ψ from the reference site to Ψ of any site remains relevant (i.e.
80 constant) over the time. For example, Taylor et al. (2010) showed that Ψ extrapolation
81 appeared to be feasible between fields despite different soil types if the general soil
82 moisture regimes were similar. Indeed, the linear relationships considered in the model did
83 break down when the soil moisture regimes or when rainfall amounts were variable
84 between the reference site and the site of prediction. Similarly, the linear relationship with
85 the reference site may be altered by irrigation (Baralon et al., 2012).

86 Because SPIDER is based on a data-based learning approach, it provides a limited formal
87 framework to explore these limitations. More specifically, it does not allow to study the
88 effect of a differentiated water input (i.e. rainfall, irrigation) on the quality of the estimates
89 produced by extrapolation from a reference site. For example, it is impossible to know if
90 there is a critical precipitation level beyond which extrapolation can no longer be applied,
91 in the same way it is difficult to know if the linear relationship is definitively lost for the
92 season after a rainfall event or if it is again possible to apply the model after a sufficiently
93 long dry period. Recent work (Gaudin et al., 2017) has shown that a mechanistic approach
94 based on a Water Balance Model (WBM) can contribute to understanding within-field
95 variations of the vine water status. These results suggest that such a modelling approach
96 might be used to study the spatial extrapolation problem by simulating the water status
97 $\Psi^{sim}(s, t)$ for several sites within the same field and by analysing how these simulated
98 dynamics relate to the one corresponding to a reference site. The main objective of this
99 paper is thus to use a vineyard dataset and a Water Balance Model to perform these
100 analyses and to provide a new angle for studying the validity of SPIDER and its limitations.

101

102 The paper is organised in three parts: i) the first will present the calibration of the WBM
103 with historical data and its validation, ii) the second will present implementation of the
104 WBM to validate the SPIDER approach based on extrapolation of simulated Ψ values from
105 a reference site and then iii) the last part will use WBM properties to better understand the
106 validity of SPIDER especially in the case of water supply either by rainfall or irrigation.

107

108 **2. Material and Methods**

109

110 **2.1. Dataset of predawn water potential observations in a Mediterranean vineyard:** 111 **Shiraz2004 and Mourvèdre2005**

112 Over the last 20 years, year 2004 and to a lesser extent 2005, were identified as the best
113 summer periods for this work. Indeed, in both these years, Languedoc experienced very
114 long periods of dry conditions interrupted by significant rainfall events. Predawn leaf water
115 potential data were collected in 2004 for one variety (Shiraz) and in 2005 for the other
116 variety (Mourvèdre) by Acevedo-Opazo et al. (2010) in vineyards of Pech Rouge (INRA
117 Gruissan, 43°08'47" N, 03°07'19" E). The 1.2 ha Shiraz vineyard was planted in 1990 (Fig.
118 1). The 1.7 ha Mourvèdre vineyard was also planted in 1990. Both are included in the *la*
119 *Clape* terroir which is classified as a designation of origin by the French authority. The
120 northern limits of this terroir follow the lower course of the river Aude and the southern
121 limits follow a former riverbed of the same river. The corresponding geological terrain is
122 Cretaceous limestone, mainly constituted of thick *Orbitolina* deposits (Lespinasse, 1982).
123 Over time, this geological material has given rise to heterogeneity in the pedological
124 material.

125 Predawn leaf water potential measurements were carried out between 3 and 5 a.m. on
126 vines located on 49 sites of the fields (Acevedo-Opazo et al., 2010). These sites were
127 defined following a regular grid as presented in Fig. 1. Measurements were made with a
128 pressure chamber (Scholander et al., 1965) at six dates either in 2004 or in 2005. The
129 pressure chamber was a Plant Water Status Console, Model 3000 (Soil moisture
130 Equipment Corp., Santa Barbara, California). One date-site data corresponds to the
131 average of three measurements on three representative vines at one site. In order to
132 perform measurements over the 49 sites in a short period of time, the following
133 organization was used: Three technicians and researchers collected the leaves and

134 brought them to a researcher (the same person for Shiraz and Mourvèdre fields) in charge
135 of measurements on the console.

136 Climatic data (Fig. 2) were monitored by the Pech Rouge weather station located 100 m
137 away from the Shiraz field (500 m away from the Mourvèdre field). These climatic data
138 were used to record rainfall events and to compute the reference evapotranspiration (ET_0)
139 according to Allen et al. (1998)

140

141 **2.2. The Spider approach for extrapolating the water status dynamics from reference** 142 **sites**

143

144 The SPIDER model was presented in Eq. 1. It was implemented on data collected in 2004
145 and 2005. Its principle is based on the (random) choice of a reference site (s_{re}). Available
146 Ψ data were used to calibrate a linear model linking the Ψ values of the reference site to Ψ
147 values of different sites in the domain. Once calibrated, as shown in Fig. 2, SPIDER can
148 be used to extrapolate any measurements taken at the reference site to each site in the
149 domain for which calibration was performed. This extrapolation uses a collection of
150 coefficients ($a_{s1}, a_{s2}, a_{s3}, \dots, a_{si}$) specific to each site of the domain ($s_1, s_2, s_3, \dots, s_i$).

151

152 **2.3 The Water Balance Model (WBM) approach for simulating Ψ dynamics**

153

154 **2.3.1 Vineyard water balance model**

155 Water balance simulation models applied to vineyards (Lebon et al., 2003; Celette et al.,
156 2010) are used in many studies and particularly in Mediterranean conditions: i) to provide
157 a diagnosis tool on vineyard water stress (Pellegrino et al., 2006), ii) to analyse the effect
158 of intercropping between vine rows (Celette et al., 2010; Ripoche et al., 2010) or iii) to
159 study irrigation needs (Gaudin and Gary, 2012; Roux et al., 2014). The main model output
160 is the dynamics of a normalized water stress index based on soil water content and called
161 Fraction of Transpirable Soil Water (FTSW). The principle of this approach is to compute
162 the daily change in soil water content from different water fluxes that occur inside the soil
163 volume accessible to vine roots. Adopting the modelling hypotheses used in Gaudin and
164 Gary (2012), the resulting update of daily FTSW, noted $FTSW_t$, can be written as:

$$165 \quad FTSW_t = \min\left(1, \max\left(0, FTSW_{t-1} + \frac{1}{FTSW} (P_t - Q_t - E_t - T_t)\right)\right) \quad [\text{Eq.2}]$$

166 In this model, the main daily water fluxes are: P_t (rain), Q_t (runoff), E_t (evaporation from
167 bare soil) and T_t (vineyard transpiration). In Gaudin and Gary (2012), Q_t is computed using

168 the NRCS Curve Number method (NRCS, 2004), Et using the FAO method (Allen et al.,
169 1998) and Tt as proposed by Lebon et al. (2003). The parameter TTSW is the Total
170 Transpirable Soil Water content.

171 The link between the FTSW modelling approach and measurements of the vine water
172 status based on predawn leaf water potential has been done by Lebon et al. (2003) and
173 Pellegrino et al. (2005) who proposed an empirical relationship which appeared robust for
174 several Mediterranean vineyard fields (Eq. 3).

$$175 \Psi \approx \Psi_{FTSW}(FTSW) = \max\left(-1.5, \frac{1}{b} \cdot \log\left(\frac{FTSW}{a}\right)\right), \text{ with } a = 1.0572, b = 5.3452 \text{ [Eq.3]}$$

176 Using Eq.2 and Eq.3 it is possible to simulate the dynamics of FTSW continuously and
177 derive an estimation $\Psi^{sim}(t)$ of water potential Ψ at time t. By limiting the simulation period
178 to the stage of vine growth corresponding to full canopy development, only a few model
179 inputs are required to implement Eq. 3. These inputs are presented in Table 1.

180

181 **2.3.2. Calibration of the model on Shiraz2004 and Mourvèdre2005**

182 In order to apply the WBM on the 49 sites of the two fields (Shiraz2004 and
183 Mourvèdre2005), values for model parameters and input variables are requested. Weather
184 variables (P_t , ET_{0t}) have been measured or derived from records from the weather station
185 but other model inputs (TTSW, CN, k_{cb} , REW, TEW, $\Psi^{sim}(0)$) have to be estimated using
186 calibration from Ψ measurements. The following calibration procedure was considered:

187

188 **Step 1:** Definition of a set of plausible values for 4 unknown inputs (all except
189 TTSW). The values selected for this work are presented in Table 2. The values in
190 Table 2 were selected from expert knowledge. They correspond to quite
191 representative values for the vineyards in the south of France and take into account
192 the diversity of cases which it is possible to meet in this region.

193

194 **Step 2:** Estimation of $k_{cb}/TTSW$ for each site of each field {Shiraz2004,
195 Mourvèdre2005} using the following approach as proposed by Gaudin et al.
196 (2017):

- 197 • Selecting measurements in dry conditions: dates {05/08, 18/08, 23/08} for
198 Shiraz2004 and {23/06, 06/07, 19/07, 05/08} for Mourvèdre2005.
- 199 • Estimating the ratio $k_{cb}/TTSW$ using the coefficient of the linear regression
200 between $\Psi^{obs}(t)$ and cumulated ET_0 on the selected dry period.

201

202 **Step3:** Optimisation of parameters $\{k_{cb}, REW, TEW, CN, \Psi^{sim}(0)\}$:

- 203 • For each site $i=1..49$ of each field {Shiraz2004, Mourvèdre2005}
- 204 • For each of the $3*3*3*7=189$ combination values defined in Table 2
- 205 ○ Computation of TTSW using $k_{cb}/TTSW$ values as estimated in Step 2
- 206 and current k_{cb} value,
- 207 ○ Computation of $\Psi^{sim}(t)$ for each parameter combination using the
- 208 WBM
- 209 ○ Computation of the mean absolute error (MAE) between simulations
- 210 and observations. The precise expression of MAE_i for n_{obs}
- 211 observations taken at times $(t_1^{obs}, \dots, t_{n_{obs}}^{obs})$ was obtained by comparing
- 212 measurements $\Psi_i^{obs,k} = \Psi_i^{obs}(t_k^{obs})$ and model predictions $\Psi_i^{sim,k} =$
- 213 $\Psi_i^{sim}(t_k^{obs})$ on a site “i” as indicated in Eq.4 :

214
$$MAE_i = \frac{1}{n_{obs}} \sum_{k=1}^{n_{obs}} |\Psi_i^{obs,k} - \Psi_i^{sim,k}| \quad [Eq.4]$$

- 215 • Selection of the set of parameters corresponding to the lowest MAE
- 216

217 Using this procedure, it was possible to obtain for each site “i” in each field: i) a continuous

218 simulation of $\Psi_i^{sim}(t)$ during the measurement period, ii) a quantification of the calibration

219 error (here the Mean Absolute Error), iii) the set of optimized model parameters.

220

221 **2.4. Methods for analysing the SPIDER approach using the Water Balance Model**

222

223 **2.4.1. Assessment of calibration performances of the WBM**

224 In order to analyse the calibration performances of the WBM applied on the 49 sites of the

225 two dataset Shiraz2004 and Mourvèdre2005, $\Psi^{sim}(t)$ was computed for each site. The

226 associated Mean Absolute Error of Calibration was then estimated using Eq. 4. For each

227 field the distribution over all sites of the obtained MAE was then analysed.

228

229 **2.4.2. Choice of the reference sites**

230 SPIDER requires the choice of a reference site in order to predict, for any site “i”, the value

231 of the potential $\Psi_i^{obs}(t_k)$ from the value observed on a reference site $\Psi_{ref}^{obs}(t_k)$. It has been

232 shown in previous studies that SPIDER prediction performances were not very sensitive to

233 the choice of the reference site (Acevedo et al., 2010; Baralon et al., 2012). It is however

234 crucial for applying the WBM that the reference site is well adjusted by model simulations.

235 In order to take this constraint into account, for each field, the reference site was chosen
 236 by taking the site with best WBM calibration error among the best sites of reference for
 237 SPIDER. By applying this procedure to each field, site 29 and site 26 were selected as
 238 reference sites respectively for Shiraz and Mourvèdre.

239

240 **2.4.3. Validating the global performances of SPIDER using WBM simulations**

241 The performance of SPIDER is measured by the prediction error. This latter as well as the
 242 linear model are defined on a small number of available observations and may therefore
 243 be biased by the limited number of measurements.

244 Using the WBM, the linear regression between the continuous dynamics of a reference
 245 site $\Psi_{ref}^{sim}(t)$ and the associated dynamics of a target site $\Psi_i^{sim}(t)$ can be computed:

246 $\hat{\Psi}_i^{sim}(t) = a_i^{sim} \cdot \Psi_{ref}^{sim}(t)$. It is therefore possible to test the prediction error of this model for
 247 each day within the measurement period. This prediction error can be seen as a
 248 generalization of the SPIDER prediction error as it also uses a linear regression model
 249 between Ψ values based on the use of a single reference site. This prediction is also more
 250 robust compared to the one based only on measurements in the sense that the number of
 251 samples is much higher (simulations are carried out every day in the measurement
 252 period). The SPIDER approach may be considered validated if the prediction errors
 253 obtained using continuous predictions of the WBM are low for most sites. In the rest of the
 254 document, the use of the data derived by the WBM to simulate the SPIDER approach as
 255 described in this section will be referred to as: WBM based regression.

256

257 **2.4.4 Theoretical analysis of SPIDER performances using the WBM in dry conditions**

258 SPIDER limitations were investigated using the WBM approach. From Gaudin et al.
 259 (2017), it is known that under dry conditions the plant water potential decreased linearly in
 260 relation to the cumulated ET_0 . Moreover, the slope of this relation can be expressed using
 261 model parameters: it is equal to the ratio of k_{cb} (basal crop coefficient) to TTSW (Total
 262 Transpirable Soil Water).

263 It is therefore possible to understand how simulated Ψ dynamics at different sites in a
 264 same field are related during a dry period. More precisely, regarding a dry period starting
 265 at time t_0 , Eq. 5 summarises changes in plant water potential for a reference site “ref” and
 266 a target site “i”.

$$\begin{aligned}
 \Psi_i^{sim}(t_0 + t) &= \Psi_i^{sim}(t_0) + \frac{k_{cb,i}}{TTSW_i} \sum_{s=t_0}^t ET_0(s) \\
 \Psi_{ref}^{sim}(t_0 + t) &= \Psi_{ref}^{sim}(t_0) + \frac{k_{cb,ref}}{TTSW_{ref}} \sum_{s=t_0}^t ET_0(s)
 \end{aligned}
 \tag{Eq.5}$$

267

268 These equations will be combined to study the relationship between spatialized simulated
269 water potentials in dry conditions.

270

271 **3. Results and Discussion**

272

273 **3.1. Calibration of WBM on historical Ψ data**

274

275 The cumulated density of calibration error of WBM is presented in Fig. 4. The error,
276 defined as the Mean Absolute Error between observations and simulations and expressed
277 in MPa, ranges from 0.03 MPa to 0.22 MPa and from 0.04 MPa to 0.25 MPa for
278 Mourvèdre2005 and Shiraz2004 respectively. 80% of the sites have an error lower than
279 0.15 MPa for Mourvèdre2005 and lower than 0.18 MPa for Shiraz2004. For each field, two
280 sites were highlighted in red in Fig. 4: sites 37 and 32 for Shiraz and sites 23 and 25 for
281 Mourvèdre. These sites were chosen to encompass the large range of calibration errors
282 from MAE = 0.05 MPa (site 37 and 23) to MAE = 0.15 MPa (sites 32 and 25). They are
283 used in Fig. 5 to illustrate the evolution dynamics of the estimated plant water potential
284 estimated from the WBM in contrasting situations (in terms of error) for the two fields. Fig.
285 5 shows a low error level of 0.05 MPa obtained on site 37 (Shiraz2004) and 23 (Mourvèdre
286 2005). Very well adjusted curves on almost all measurements are associated to this low
287 error level. A moderate error level of 0.15 MPa is obtained on site 32 (Shiraz2004) and 25
288 (Mourvèdre2005). For such sites, the model does not adjust properly to all measurement
289 dates. Higher deviations between outputs of the model and observed values are noticed at
290 the beginning of the measurement period for site 32 (Shiraz2004) while over and under
291 estimations are observed over the whole experimentation period for site 25
292 (Mourvèdre2005).

293 As seen in Fig. 4, the calibration is globally better on Mourvèdre2005 than on Shiraz2004,
294 and overall these error levels are considered acceptable to use the model for the spatial
295 extrapolation problem.

296

297 **3.2. Validation of the SPIDER model on historical Ψ data**

298

299 Fig. 6 shows a comparison between errors observed with SPIDER and WBM based
300 regression. For Mourvèdre2005, the prediction error using the WBM-based regression is
301 low (<0.15 MPa for 90% of sites) and close to error values obtained with SPIDER. For
302 Shiraz2004, 80% of the sites have a prediction error lower than 0.15 MPa. (Note that the

303 remaining 20% are also characterized by higher calibration errors: the model does not
304 adjust at its best and the WBM-based regression results are thus less significant on these
305 sites.)

306 Overall, the prediction error of the WBM-based regression appears low for both fields. This
307 means that the knowledge of the simulated Ψ dynamics on a reference site allows to
308 predict with relatively high precision the simulated Ψ dynamics on a target site using the
309 simple linear regression model $\widehat{\Psi}_i^{sim}(t) = a_i^{sim} \cdot \Psi_{ref}^{sim}(t)$. This result strengthens the
310 validity of SPIDER: indeed, it shows that the linear regression model based on several ψ
311 measurements (SPIDER) is also valid when considering simulated Ψ dynamics at any day
312 within the measurement period. This is one significant result of the present paper.

313
314 Fig. 7 allows to analyse the results obtained with linear predictions from an observed or
315 simulated reference site more precisely. It shows the simulated Ψ dynamics for two sites:
316 sites 37 (Shiraz2004) and 23 (Mourvèdre2005). Both sites present a low calibration error
317 (see Fig. 4) and a low prediction error using the WBM-based regression (0.11 MPa for site
318 37 and 0.03 MPa for site 23). The regression line (in grey) is therefore in both cases an
319 accurate way to predict $\Psi_i^{sim}(t)$ (grey circles) from $\Psi_{ref}^{sim}(t)$. It can be noted in Fig. 7 that
320 while the linear model is a good approximation of the link between Ψ dynamics, this
321 relationship may present some complex features: for site 23 (Mourvèdre2005), non-
322 linearity is observed for low Ψ values. For site 37 (Shiraz2004) the relationship between Ψ
323 values is mostly piecewise linear. Different correlations seem to apply at different periods
324 with the same slope but different intercepts. These properties will be further analysed in
325 the following section.

326

327 **3.3. Theoretical analysis of SPIDER performances in dry conditions**

328 The previous results have shown that the WBM approach was able to validate the SPIDER
329 results on the two-year data set. This section aims at using the WBM in order to gain more
330 insights into the SPIDER conditions of application. To this aim both dry and wet conditions
331 were considered.

332

333 **3.3.1. Dry conditions: piecewise linearity**

334 From Eq.5 and using the simple trick that $ax + b = \frac{a}{c} \cdot (cx + d) + b - \frac{ad}{c}$ (for any $c \neq 0$), the
335 following relationship (Eq.6) between simulated Ψ values can be obtained under dry
336 conditions:

$$337 \quad \Psi_i^{sim}(t_0 + t) = \left(\frac{k_{cb,i} \cdot TTSW_{ref}}{k_{cb,ref} \cdot TTSW_i} \right) \Psi_{ref}^{sim}(t_0 + t) + \Psi_i^{sim}(t_0) - \left(\frac{k_{cb,i} \cdot TTSW_{ref}}{k_{cb,ref} \cdot TTSW_i} \right) \Psi_{ref}^{sim}(t_0) \quad [\text{Eq.6}]$$

338 Eq. 6 can be written as follows:

$$339 \quad \Psi_i^{sim}(t_0 + t) = a_i^{param} \cdot \Psi_{ref}^{sim}(t_0 + t) + b_i^{param,t_0} \quad [\text{Eq.7}]$$

$$340 \quad \text{with } \begin{cases} a_i^{param} = \left(\frac{k_{cb,i} \cdot TTSW_{ref}}{k_{cb,ref} \cdot TTSW_i} \right) \\ b_i^{param,t_0} = \Psi_i^{sim}(t_0) - a_i^{param} \cdot \Psi_{ref}^{sim}(t_0) \end{cases}$$

341 Eq.7 shows that every dry period starting at $t=t_0$ results, for $t>t_0$ and under dry conditions,
 342 in a linear relation between $\Psi_i^{sim}(t)$ and $\Psi_{ref}^{sim}(t)$. The slope of this relation a_i^{param} is
 343 defined using basal crop coefficients and TTSW of each site and does not depend on the
 344 water status at $t=t_0$, unlike the intercept b_i^{param,t_0} . This property explains the piecewise
 345 linearity that can be seen in Fig.7a: there are clearly two periods of piecewise linearity in
 346 this simulation.

347

348 3.3.2. Persistent dry conditions: stable linearity

349 When dry conditions last a long time under high evaporative demand (high ET_0), the model
 350 can be simplified. In such cases, the water potential reaches very low values and it is
 351 possible to neglect the influence of the intercept in the relationships between Ψ dynamics
 352 (Eq. 8).

$$353 \quad \begin{aligned} \Psi_i^{sim}(t_0 + t) &= \Psi_i^{sim}(t_0) + \frac{k_{cb,i}}{TTSW_i} \sum_{s=t_0}^t ET_0(s) \approx \frac{k_{cb,i}}{TTSW_i} \sum_{s=t_0}^t ET_0(s) \\ \Psi_{ref}^{sim}(t_0 + t) &= \Psi_{ref}^{sim}(t_0) + \frac{k_{cb,ref}}{TTSW_{ref}} \sum_{s=t_0}^t ET_0(s) \approx \frac{k_{cb,ref}}{TTSW_{ref}} \sum_{s=t_0}^t ET_0(s) \end{aligned} \quad [\text{Eq.8}]$$

354 In these specific conditions, this implies that $\Psi_i^{sim}(t_0 + t) \approx a_i^{param} \cdot \Psi_{ref}^{sim}(t_0 + t)$. The linear
 355 relation is therefore mainly characterized by only basal crop coefficients and TTSW of
 356 each site, which is likely to be stable over several years.

357

358 3.3.3. Link between the regression coefficient and model parameters

359 Based on the previous section, a_i^{param} is known to drive the relationship between
 360 simulated Ψ dynamics during persistent dry conditions. In Fig. 8, a comparison between
 361 a_i^{param} and the regression coefficient a_i^{sim} of the predictive model using simulations
 362 (defined by $\widehat{\Psi}_i^{sim}(t) = a_i^{sim} \cdot \Psi_{ref}^{sim}(t)$) is performed to evaluate if a_i^{param} can be a good
 363 estimate of a_i^{sim} even if the whole period does not correspond to dry conditions.

364 Both coefficients have been computed for each site in each field (a_i^{param} was computed
 365 from the calibrated model parameters, a_i^{sim} by linear regression on simulations).

366 Remember that 49 sites are available in each field. The site of reference being removed,
367 this approach results in a comparison of 48 values for each field.

368 a_i^{param} appears to be a good approximation of a_i^{sim} for both data sets Shiraz2004 and
369 Mourvèdre2005 even if the weather conditions were not persistently dry (Fig. 8). On
370 condition that k_{cb} and TTSW are stable over several years (which happens if the vine
371 grower does not significantly change any management practices in the vineyard) and that
372 climatic conditions are globally the same (dominantly dry), this implies that the linear
373 relationship between simulated Ψ values should be globally stable over the years and
374 related to model parameters k_{cb} and TTSW.

375

376 **3.4. Impact of rainfall events on prediction quality in historical Ψ data**

377

378 The WBM approach allows to better study the limitation of SPIDER especially during and
379 after a rainfall event or in case of irrigation. It should be noted that studying these
380 situations is difficult with an empirical approach such as SPIDER since it would require
381 performing a large number of measurements over limited periods of time. The
382 implementation of an approach based on a validated WBM (under the conditions of the
383 study) allows a more detailed study.

384 This analysis was made numerically on the two datasets using the methodology presented
385 in Fig. 9 by focusing on the ratio of simulation Ψ dynamics for every t in the measurement

386 period $\frac{\Psi_i^{sim}(t)}{\Psi_{ref}^{sim}(t)}$ and on the regression coefficient a_i^{sim} derived from the WBM based
387 regression ($\widehat{\Psi}_i^{sim}(t) = a_i^{sim} \cdot \Psi_{ref}^{sim}(t)$). The normalized distance $d_i(t)$ between this ratio of
388 simulated Ψ and the regression coefficient was computed for each site i as is Eq.9:

$$389 \quad d_i(t) = \frac{1}{a_i^{sim}} \cdot \left(\frac{\Psi_i^{sim}(t)}{\Psi_{ref}^{sim}(t)} - a_i^{sim} \right) \quad [\text{Eq.9}]$$

390 Finally, in order to aggregate the results for all sites, quantiles {10%,90%} of the $d_i(t)$
391 distribution were computed. They are studied as a function of time to see how the local
392 linearity between Ψ dynamics is broken by rainfall or irrigation events. Indeed, the periods
393 where the linear approximation works well (resp. poorly) correspond to low (resp. high)
394 $d_i(t)$ values. Another point of interest is to look for recovery periods after a rainfall or
395 irrigation event after which Ψ dynamics are again linearly correlated.

396

397 The assessment of the robustness of the linear approximation between Ψ dynamics is
398 presented in Fig. 10. The prediction using a linear regression model has been shown to be

399 globally acceptable in Fig. 6, but it can be seen in Fig. 10 that rainfall alters the linearity of
400 the relationship locally and that the interference is linked to the amount of rainfall. The
401 impact of rainfall events is however not uniform even for a same amount of water: the
402 heaviest rainfalls (for example the 20 mm rainfall on Shiraz2004) may not change the
403 relationship for some sites while altering it for others. On the other hand, many small
404 rainfall events (those <5 mm) do not change the quality of the linear prediction, probably
405 because the corresponding incoming water is evaporated very quickly. However, the main
406 property stressed by Fig. 10 is the presence of a recovery time before regaining the
407 previous quality of the linear model approximation, including after the heaviest rainfalls: the
408 prediction using the linear model becomes accurate again after a certain time (see, for
409 example, the 20 mm rainfall on Shiraz2004 and the decreasing of the error after this
410 event).

411 This result is particularly significant and provides practical information for using an
412 empirical approach like SPIDER. It shows that SPIDER could still be applied even after
413 rainfall events or irrigation. After such events, there is transitory period during which any
414 extrapolation of water status values observed on the site of reference would lead to biased
415 estimations. However, SPIDER becomes relevant again after a certain period of time. For
416 these experimentations, a period of 5 days would have been sufficient for most sites after
417 a small rainfall event (<15mm) while a period of 15 days would have been required for
418 heavier rainfall (>15mm). Naturally, further experiments will be necessary to validate this
419 recommendation for its use on a larger scale.

420

421 **4. Conclusion**

422

423 This paper analyses why the vine water status, as characterized by predawn water
424 potential values, can be extrapolated from measurements on a single reference site using
425 a linear regression model known as the SPIDER approach. To perform this analysis, a
426 water balance model running on a daily basis was used to provide daily estimates of
427 predawn water potential values. The model was calibrated and used on two datasets
428 (different vineyards, different years) with 49 sites of predawn leaf water potential
429 measurements.

430

431 The use of the water balance model confirmed that predawn water potential values at any
432 site can be estimated from observations performed on a reference site using a linear
433 regression model linking the two dynamics with a low error level. For persistent dry

434 conditions occurring frequently in Mediterranean vineyards, the ratio of simulated predawn
435 water potential values was shown to be simply linked to model parameters (basal crop
436 coefficient and Total Transpirable Soil Water) indicating that the linear relationship between
437 simulated water potential dynamics is stable over several years provided persistent dry
438 conditions are dominant. Finally, the robustness of the relationship to rainfall or irrigation
439 events was analysed using the water balance model. This demonstrated that the
440 relationship between the simulated water potential dynamics is less predictive around a
441 rainfall event but that its quality is recovered after a period of time if no other rain event
442 occurs. This study demonstrates the relevance of spatial extrapolation of the vine water
443 status from a reference site with a linear regression model with new insights on the
444 properties of the predictions. This study confirms the interest of its application in viticulture
445 either at the within-field level or at larger scale.

446

447 **5. Acknowledgements**

448 We thank Hernan Ojeda and Nicolas Saurin (INRA Gruissan) for sharing vineyards data.

449

450 **6. References**

451

452 Acevedo-Opazo, C., Tisseyre, B., Ojeda, H., Ortega-Farias, S., Guillaume, S., 2008. Is it
453 possible to assess the spatial variability of vine water status? *Journal International des*
454 *Sciences de la Vigne et du Vin* 42(4), 203-219.

455

456 Acevedo-Opazo, C., Tisseyre, B., Ojeda, H., Guillaume, S., 2010. Spatial extrapolation of
457 the vine (*Vitis vinifera* L.) water status: A first step towards a spatial prediction model.
458 *Irrigation Science* 28, 143-155.

459

460 Allen, R.G., Pereira, L.S., Raes, D., Smith, M., 1998. Crop evapotranspiration. Guidelines
461 for computing crop water requirements. Irrigation and drainage paper 56, FAO, Roma.

462

463 Baralon, K., Payan, J.C., Salançon, E., Tisseyre, B., 2012. Spider: Spatial extrapolation of
464 the vine water status at the whole denomination scale from a reference site. *Journal*
465 *International des Sciences de la Vigne et du Vin* 46(3), 167-175.

466

467 Brillante, L., Mathieu, O., Lévêque, J., van Leeuwen, C., Bois, B., 2018. Water status and
468 must composition in grapevine cv. Chardonnay with different soils and topography and a
469 mini meta-analysis of the $\delta^{13}\text{C}$ / water potentials correlation. *Journal of the Science of Food
470 and Agriculture* 98, 691-697.

471

472 Celette, F., Ripoche, A., Gary, C., 2010. WaLIS– A simple model to simulate water
473 partitioning in a crop association: The example of an intercropped vineyard. *Agricultural
474 Water Management* 97, 1749-1759.

475

476 Dry, P.R., Loveys, B.R., 1998. Factors influencing grapevine vigour and the potential for
477 control with partial rootzone drying. *Australian Journal of Grape and Wine Research* 4,
478 140-148.

479

480 Gaudin, R., Gary, C., 2012. Model-based evaluation of irrigation needs in Mediterranean
481 vineyards. *Irrigation Science* 30, 449-459.

482

483 Gaudin, R., Roux, S., Tisseyre, B., 2017. Linking the transpirable soil water content of a
484 vineyard to predawn leaf water potential measurements. *Agricultural Water Management*
485 182, 13-23.

486

487 Lebon, E., Dumas, V., Pieri, P., Schultz, H.R., 2003. Modelling the seasonal dynamics of
488 the soil water balance of vineyards. *Functional Plant Biology* 30, 679-710.

489

490 Lespinasse, P., 1982. Notice explicative de la feuille géologique Narbonne 1/50 000.
491 BRGM, Orléans.

492

493 NRCS, 2004. *National Engineering Handbook*. Chapter 10: Estimation of Direct Runoff
494 from Storm Rainfall.

495

496 Ojeda, H., Andary, C., Kraeva, E., Carbonneau, A., Deloire, A., 2002. Influence of pre- and
497 postveraison water deficit on synthesis and concentration of skin phenolic compounds
498 during berry growth of *Vitis vinifera* cv. Shiraz. *American Journal of Enology and Viticulture*
499 53, 261-267.

500

501 Pellegrino, A., Lebon, E., Simonneau, T., Wery, J., 2005. Towards a simple indicator of
502 water stress in grapevine (*Vitis vinifera* L.) based on the differential sensitivities of
503 vegetative growth components. Australian Journal of Grape and Wine Research 11, 306-
504 315.

505

506 Pellegrino, A., Gozé, E., Lebon, E., Wery, J., 2006. A model-based diagnosis tool to
507 evaluate the water stress experienced by grapevine in field sites. European Journal of
508 Agronomy 25, 49-59.

509

510 Rezaei, J.H., Reynolds, A.G., 2010. Impact of vine water status on sensory attributes of
511 Cabernet franc wines in the Niagara peninsula of Ontario. Journal International des
512 Sciences de la Vigne et du Vin 44(6), 61-75.

513

514 Ripoche, A., Celette, F., Cinna, J.P., Gary, C., 2010. Design of intercrop management
515 plans to fulfil production and environmental objectives in vineyards. European Journal of
516 Agronomy 32, 30-39.

517

518 Roux, S., Delpuech, X., Daudin, G., Brun, F., Wery, J., Wallach D., 2014. Providing user
519 oriented uncertainty information with a vineyard model used for irrigation decisions.
520 Volume 6 of the Advances in Agricultural System Modeling. Pract. Appl. Agric. Syst.
521 Models Optim. Use Ltd. Water, 5 (2014), pp. 183-208

522

523 Scholander, P.F., Hammel, H.T., Bradstreet, E.D., Hemmingsen, E.A., 1965. Sap
524 pressure in vascular plants. Science 148, 339-346.

525

526 Séguin, G. 1983. Influence des terroirs viticoles sur la constitution et la qualité des
527 vendanges. Bulletin de l'O.I.V. 56, 3-18.

528

529 Taylor, J.A., Acevedo-Opazo, C., Ojeda, H., Tisseyre, B., 2010. Identification and
530 significance of sources of spatial variation in grapevine water status. Australian Journal of
531 Grape and Wine Research 16, 218-226.

532

533 Tregoat, O., Van Leeuwen, C., Choné, X., Gaudillère, J.P., 2002. Etude du régime
534 hydrique et de la nutrition azotée de la vigne par des indicateurs physiologiques. Influence

535 sur le comportement de la vigne et la maturation du raisin (*Vitis vinifera* L. cv Merlot,
536 2000, Bordeaux). Journal International des Sciences de la Vigne et du Vin 36(3), 133-142.

537

538 Van Leeuwen, C., Seguin, G., 1994. Incidences de l'alimentation en eau de la vigne
539 appréciée par l'état hydrique du feuillage sur le développement végétatif et la maturation
540 du raisin (*Vitis vinifera* variété Cabernet franc, Saint-Emilion 1990). Journal International
541 des Sciences de la Vigne et du Vin 28(2), 81-110.

542

543 Van Leeuwen, C., Tregoat, O., Choné, X., Bois, B., Pernet, D., Gaudillère, J.P., 2009. Vine
544 water status is a key factor in grape ripening and vintage quality for red Bordeaux wine.
545 How can it be assessed for vineyard management purposes? Journal International des
546 Sciences de la Vigne et du Vin 43(3), 121-134.

547

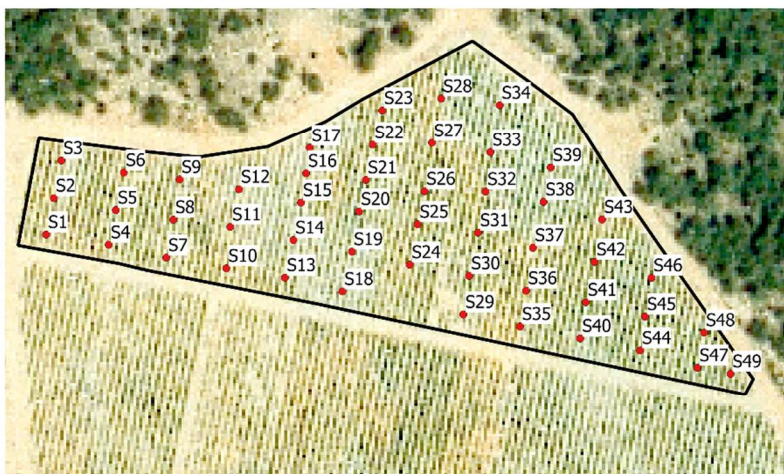
548

549

550



a)



b)

Fig. 1. Map of Shiraz (a) and Mourvèdre (b) fields and their 49 measurement sites (Pech Rouge, INRA Grissan, 43°08'47" N, 03°07'19" E).

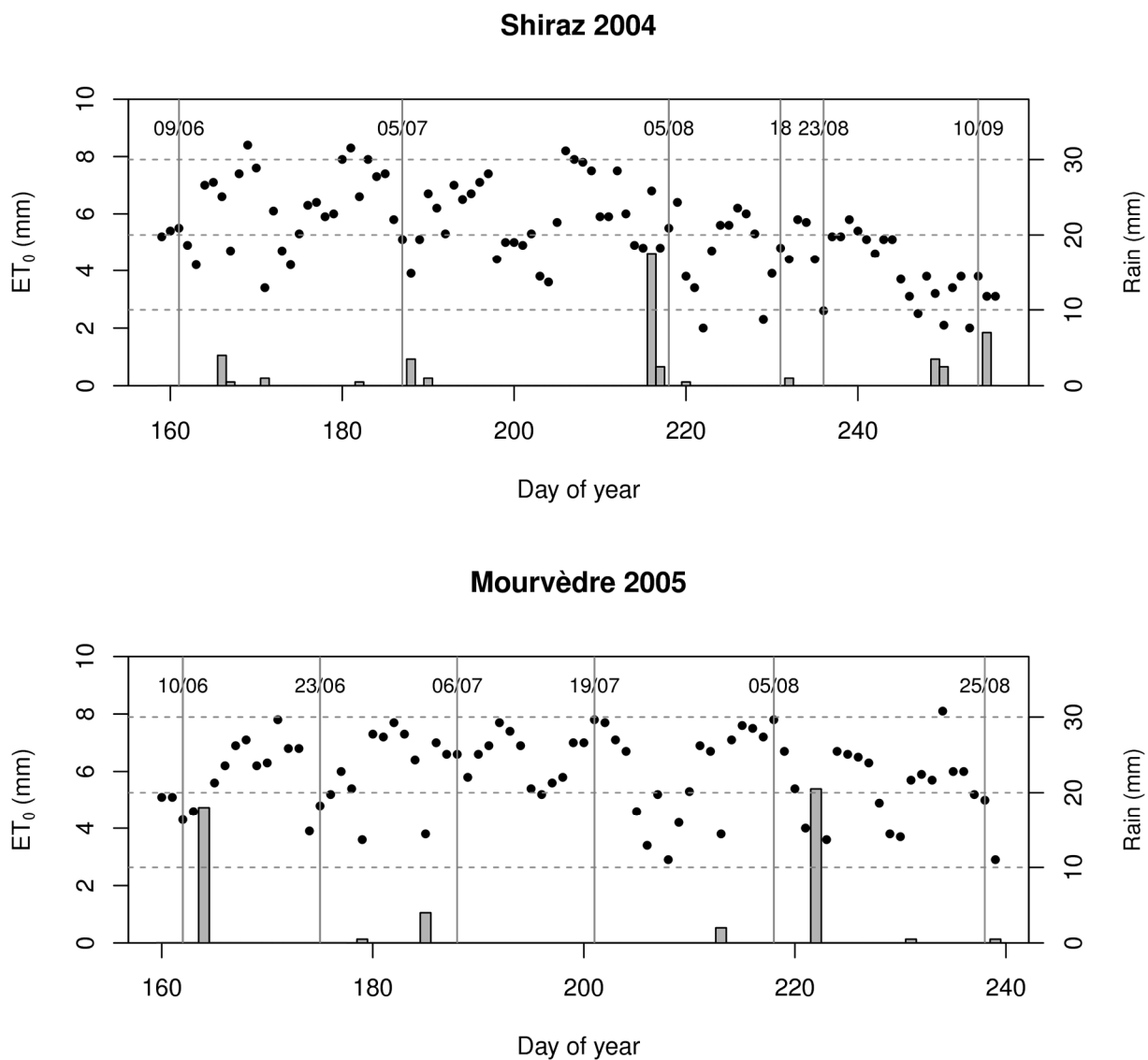


Fig. 2. Climatic data: Rainfall (grey bars) and Evapotranspiration (black dots) measured on the two fields Shiraz 2004 and Mourvèdre 2005 respectively between June-September 2004 and June-September 2005. Measurement dates of Predawn leaf water potential are indicated as vertical lines for each field.

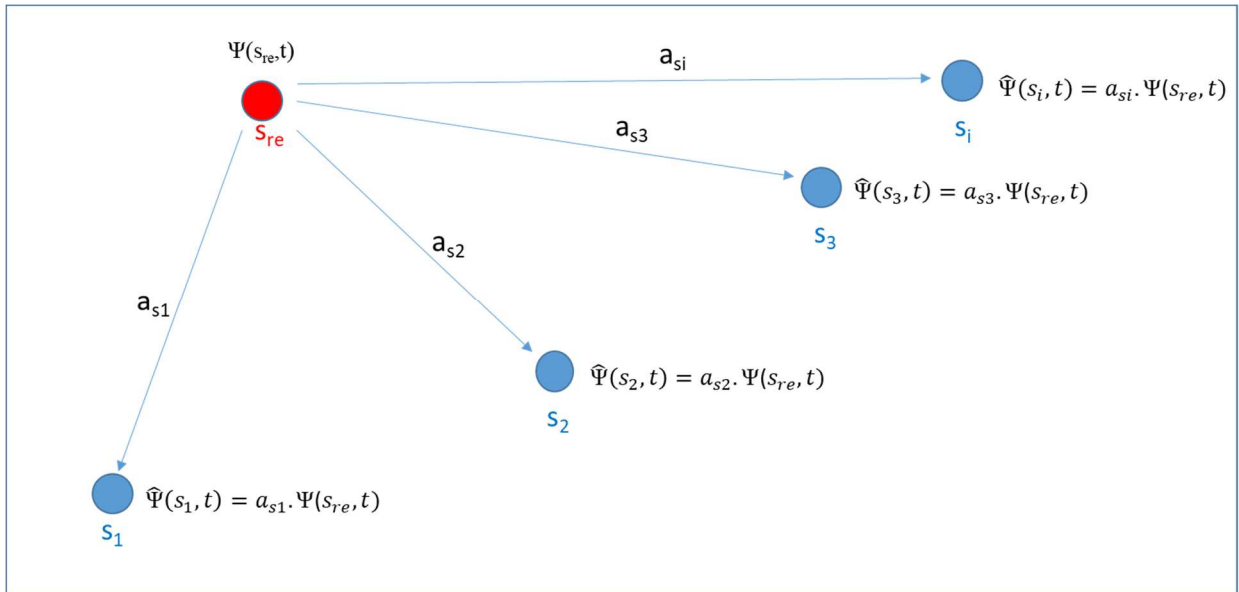


Fig. 3. The principle of the empirical approach SPIDER where the plant water potential ($\Psi(s_{re}, t)$) measured at a reference site is linearly extrapolated to other locations ($s_1, s_2, s_3, \dots, s_i$) of the field using site-specific coefficients ($a_{s1}, a_{s2}, a_{s3}, \dots, a_{si}$) to provide estimates of plant water status ($\Psi(s_1, t), \Psi(s_2, t), \Psi(s_3, t), \dots, \Psi(s_i, t)$) on unsampled locations at the same date t .

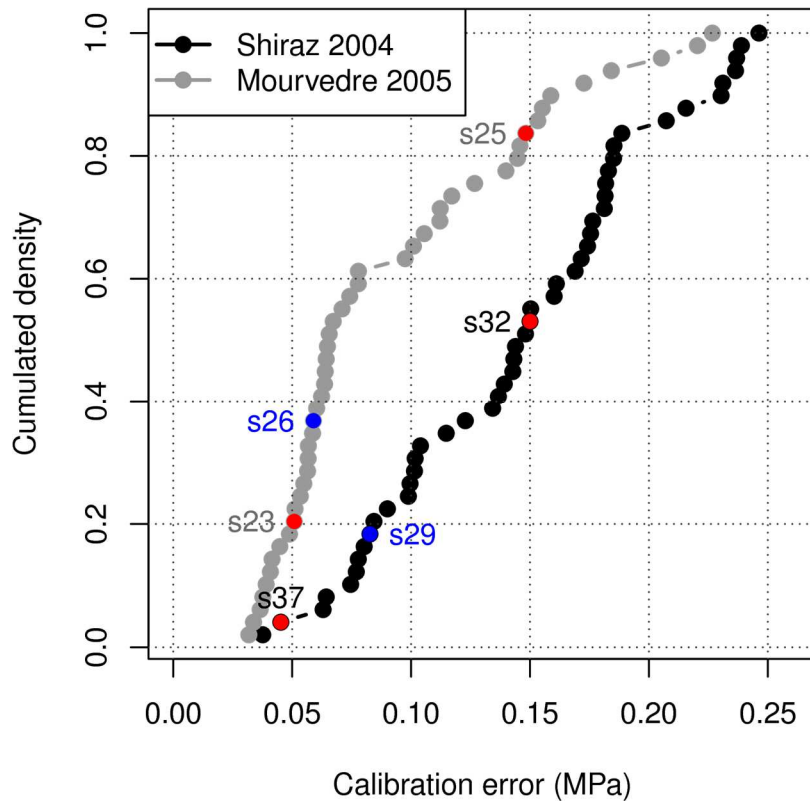


Fig. 4. The cumulative distribution of calibration errors (Mean Absolute Errors) of the model on the 49 sites in the two fields (sites in red are subjected to more detailed analysis presented in Fig. 5, and sites in blue are reference sites)

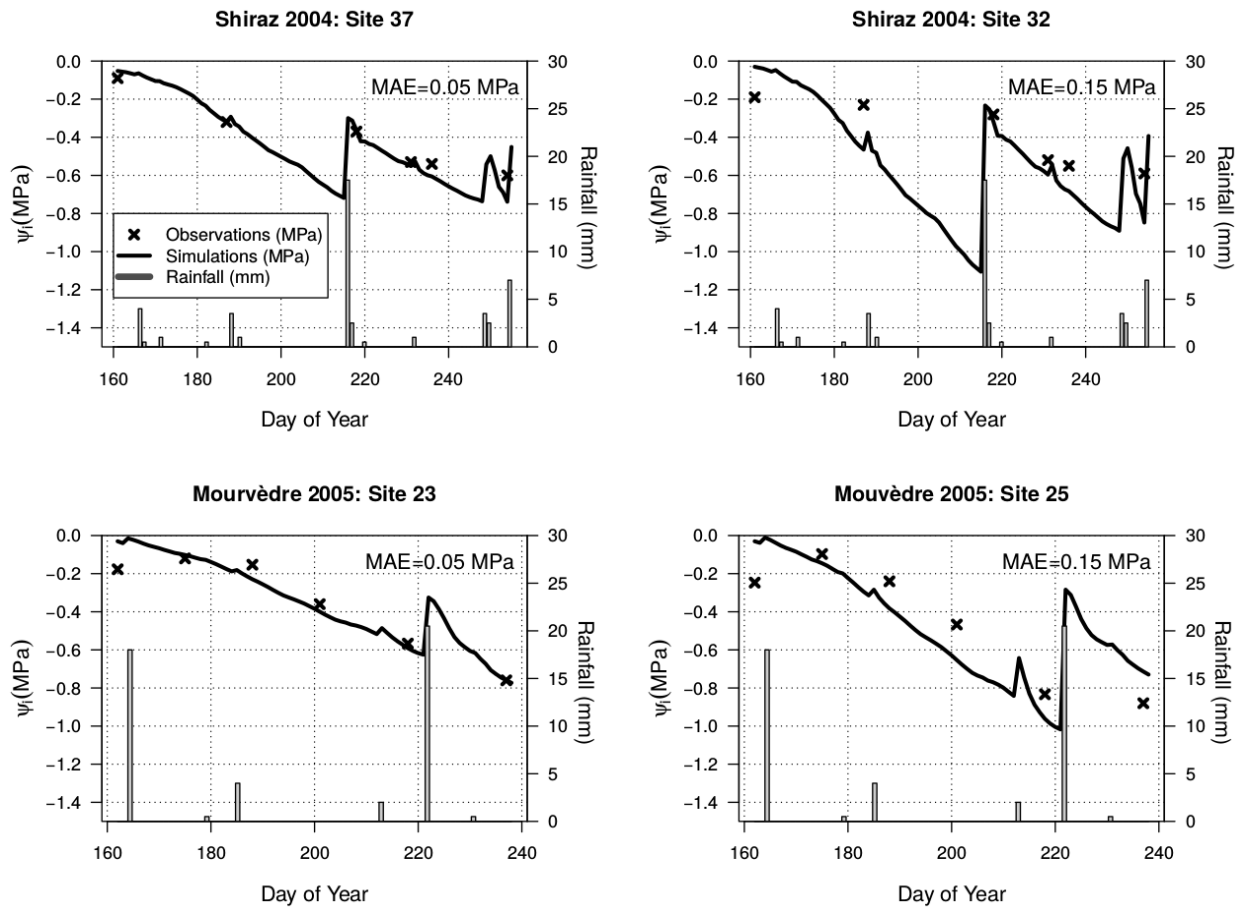


Fig. 5. Detailed analysis of the water balance model showing estimated and observed Ψ values for 2 sites of each field Shiraz2004 and Mourvèdre 2005. Sites were chosen to encompass the large range of calibration errors from MAE =0.05 MPa (site 37 and 23) to MAE = 0.15 MPa (sites 32 and 25).

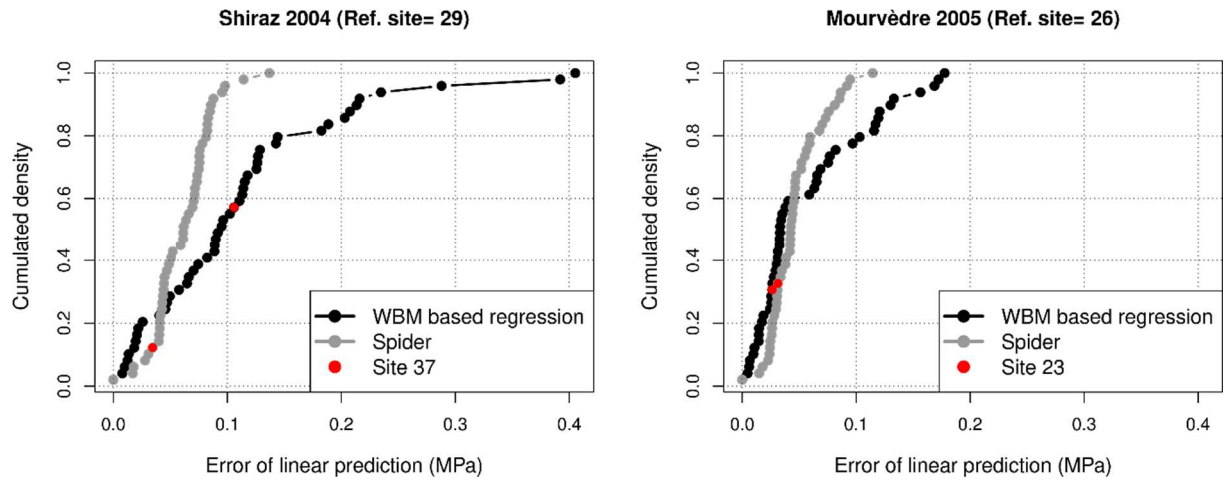


Fig. 6. Cumulative distribution errors (Mean Absolute Errors of Prediction, MPa) for SPIDER and for the WBM based regression. Result obtained on field Shiraz2004 are presented on the left and those obtained on Mourvèdre2005 on the right (the two sites are more precisely analysed in Fig. 7).

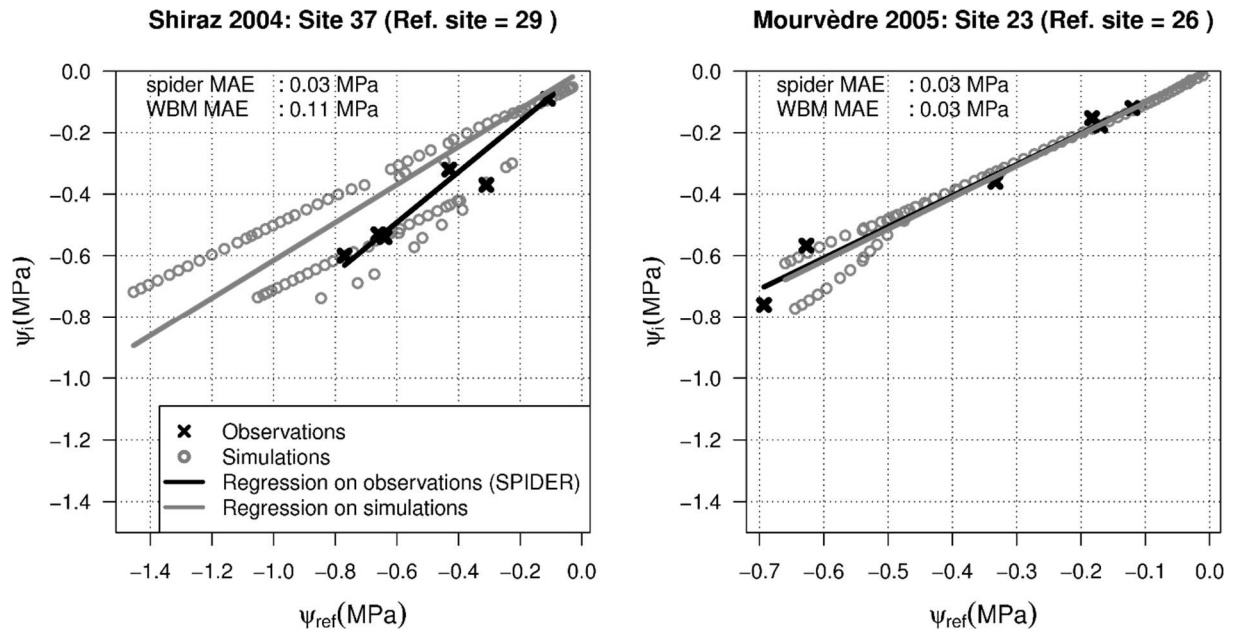


Fig. 7. The comparison of predictions obtained from a reference site with SPIDER and with the WBM-based regression for two sites.

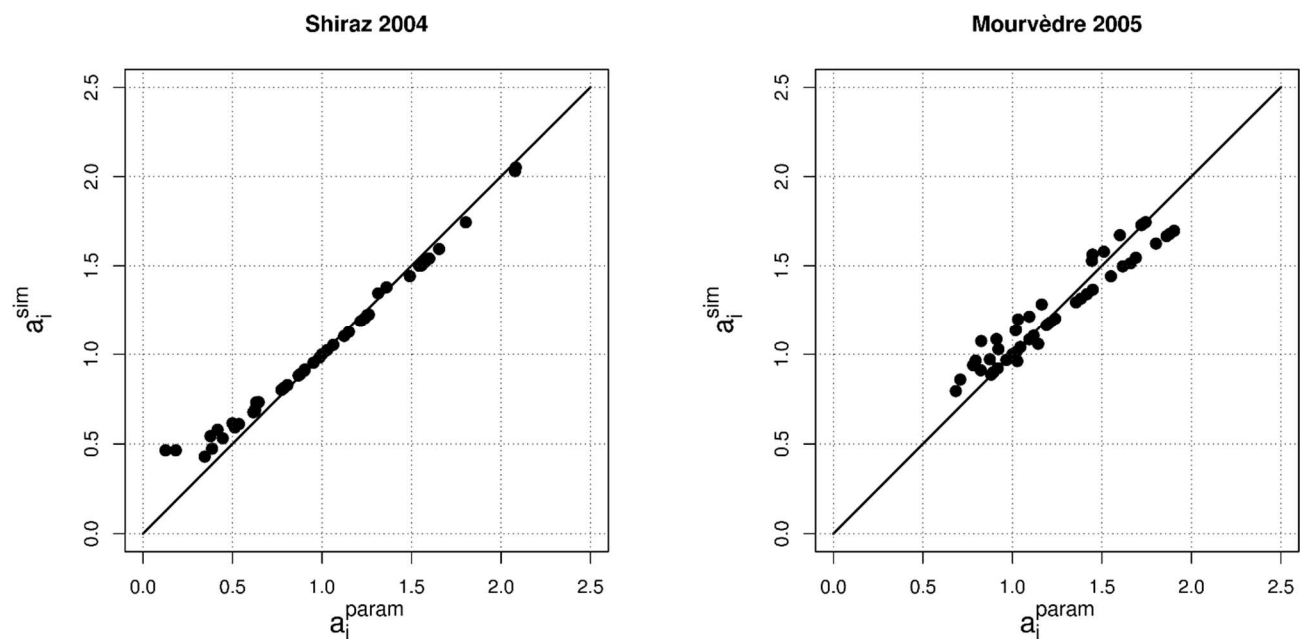


Fig. 8. The comparison of a_{sim}^i (coefficient of the WBM based regression) and a_i^{param} (derived from the WBM parameters k_{cb} and TTSW).

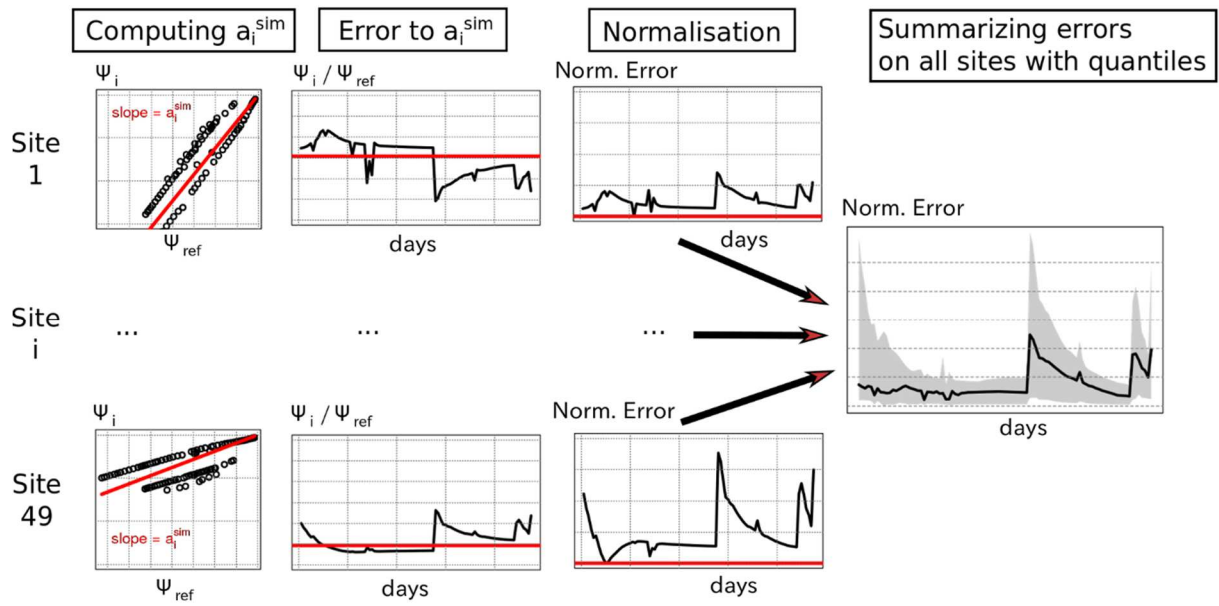


Fig. 9. Methodology used to analyse the impact of rain events on the quality of linear predictive model $\hat{\Psi}_i^{sim}(t) = a_i^{sim} \cdot \Psi_{ref}^{sim}(t)$. First the regression coefficients a_i^{sim} are computed, then an error is defined between the ratio of water potentials and the regression coefficient. This error is normalized in order to study its quantiles when aggregating the results on all 49 sites. The final results obtained for each field are presented in Fig. 10 and linked to climatic data.

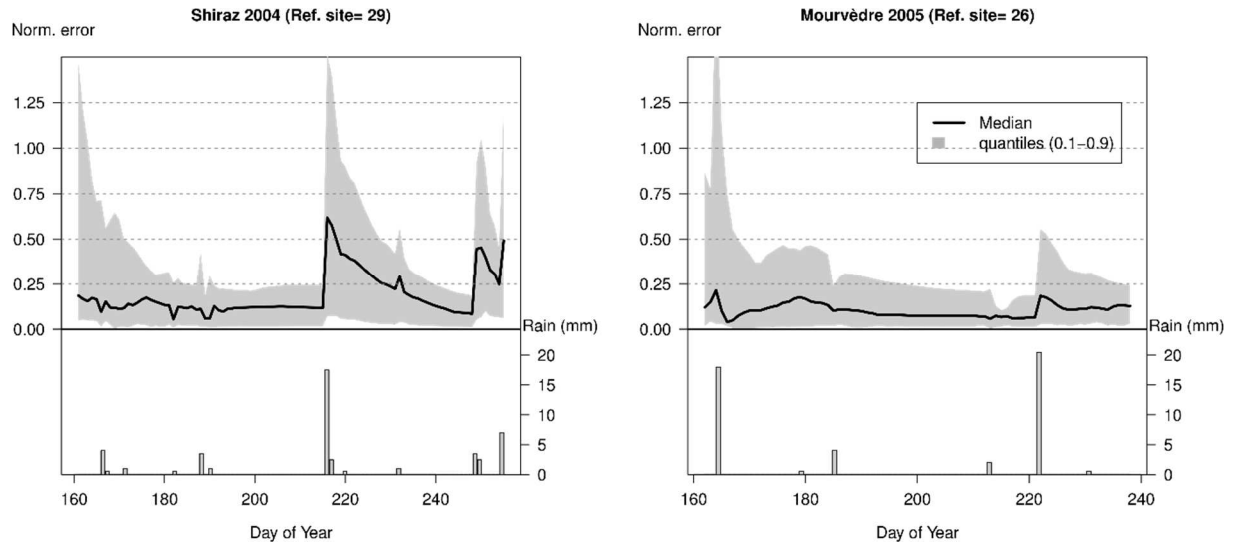


Fig. 10. Analysis of the temporal quality of the linear predictive model $\widehat{\Psi}_i^{sim}(t) = a_i^{sim} \cdot \Psi_{ref}^{sim}(t)$ using the quantiles of the normalized error $d_i(t) = \frac{1}{a_i^{sim}} \left(\frac{\Psi_i^{sim}(t)}{\Psi_{ref}^{sim}(t)} - a_i^{sim} \right)$. The median (in black) and quantiles (in grey) of the distribution of distances are plotted against time along with the distribution of rainfall.

Table 1: Water Balance Model inputs when limiting simulation to the full canopy development stage

Model Input name	Type of input	Definition	Unit
$\Psi^{sim}(0)$	Initial state	Vine water potential at simulation start	MPa
TTSW	Parameter	Total Transpirable Soil Water	mm
K _{cb}	Parameter	Basal crop coefficient	-
CN	Parameter	Curve Number for runoff module	-
(REW,TEW)	Parameter	Readily and Total evaporable water	(mm,mm)
ET _{0t}	input variable	Daily reference evapotranspiration	mm
P _t	input variable	Daily rain	mm

Table 2: domain definition of the set of tested values for four model parameters

Parameter	Tested values
k_{cb}	{0.45; 0.5; 0.55}
(REW,TEW)	{(3,7); (5,12); (9,20)}
CN	{70, 80, 90}
$\Psi^{sim}(0)$	{ $\Psi_{FTSW}(0.3), \Psi_{FTSW}(0.4), \dots, \Psi_{FTSW}(0.9)$ }